Studies of spectroscopy and cyclic voltammetry on a zirconium hexacyanoferrate modified electrode

ARTICLE *in* JOURNAL OF ELECTROANALYTICAL CHEMISTRY · APRIL 2001

Impact Factor: 2.87 · DOI: 10.1016/S0022-0728(00)00543-X

3 AUTHORS, INCLUDING:

Shou-Qing Liu
Suzhou University of Science and Technol…

24 PUBLICATIONS **372** CITATIONS

SEE PROFILE

A New Family of Dendrimers with Naphthaline Core and Triphenylamine Branching as a Two-Photon Polymerization Initiator

Xiaomei Wang,*,† Feng Jin,† Zhigang Chen,† Shouqing Liu,† Xiaohong Wang,† Xuanming Duan,*,‡ Xutang Tao,*,§ and Minhua Jiang§

Key Laboratory of Environmental Functional Materials of Jiangsu Province and Suzhou City, Institute of Chemistry and Bioengineering, Suzhou University of Science and Technology, Suzhou, 215009, China, State Key Laboratory of Crystal Materials, Shandong University, Jinan, 250100, China, and Key Laboratory of Functional Crystals and Laser Technology, Technical Institute of Physics and Chemistry, Chinese Academy of Sciences, Beijing, 100080, China

Received: August 26, 2010; Revised Manuscript Received: November 10, 2010

A new family of dendrimers with a naphthaline-core flanked on both sides by triphenylamine-branching was successfully synthesized and presented an increasing two-photon absorption (TPA) cross section from 959 to 9575 GM with the generation number from **1** to **3**. These dendrimers can efficiently initiate the acrylate resins to polymerization to obtain very regular diamond structures and display higher two-photon polymerization (TPP) efficiency and sensitivity with the generation number. The overall TPP processes involved in two-photon excitation, intramolecular charge transfer, and intramolecular energy transfer as well as intermolecular electron transfer between initiator and monomer are described. Steady-state fluorescence and time-resolved decay dynamics revealed that the light energy was absorbed by peripheral triphenylamine unit and then transferred to generation **1**, the energy funnel. Although strong interaction between dendritic initiator and monomer has been observed based on fluorescence quenching measurements, no intermolecular energy transfer but electron transfer is confirmed by the cyclic voltammograms and HOMO−LUMO measurements. That is, the dendritic initiator first produces the excited state via two-photon absorption, then transfers an electron to an acrylate monomer, and finally induces the later to polymerize.

Introduction

Conjugated dendrimers can provide an effective architectural strategy for the purpose of significant enhancement in two-photon absorption (TPA)[1−7] due to their large intramolecular charge transfer.[8] The advantaged characteristics[9,10] that TPA can confine in a very small volume (several nanometers) and penetrate deeply within three-dimensional medium are especially suitable for the microfabrication according to two-photon polymerization (TPP).[13−16] At present, highly efficient TPP initiators[17−20] were intensively researched since the conventional ultraviolet (UV) active initiators are limited in two-photon polymerization due to their poor TPA near-infrared regions. It was known that increasing molecular dimension is a good strategy to improve TPA,[21−25] and the branched molecule containing acceptor group (A) usually possesses low fluorescence yield and high triplet quantum yield, which endow the initiator with high sensitivity and low threshold of two-photon polymerization.[17,19,26−28] Extrapolating this idea, one might conclude that chromophores with more acceptor substituents are suitable for TPP initiator.[20] However, some other reports[29−31] show that the D-π-D chromophores also act as efficient TPP initiators. The influences of structural parameters upon TPP initiation efficiency and sensitivity as yet need to be investigated deeply. Lots of papers concerning TPP initiators based on symmetrical, asymmetrical, and even branching motifs have been published,[17−31] but few reports have published the dendritic D-π-D initiators with the generation effect to our knowledge. Since treelike dendritic structures based on identical branched repeat units present promising light harvesting, the absorbed light energy can be efficiently transferred to a molecular trap in the center of a dendrimer to be used for photochemical reaction.[32−34] Due to these unique properties, dendrimers with D-π-D architecture can be attractive candidates for two-photon induced initiator. We have now designed and synthesized a series of D-π-D dendritic chromophores and investigated the generation effect on TPP efficiency. As shown in Scheme 1, the smallest chromophore Np-G**1**, regarded as generation **1**, is the molecule with a naphthaline-core flanked on both sides by one triphenylamine group. Similarly, generation **2** (named as Np-G**2**) and **3** (named as Np-G**3**) are the naphthaline derivatives containing three and seven triphenylamine units on both sides, respectively. As for Np-G**1.5** and Np-G**2.5** (regarded as generation **1.5** and **2.5**, respectively), both are the molecules appended two and four triphenylamine units on two sides, respectively (structures not presented).

Experimental Section

Measurements. Electron impact (mode laser) mass spectra and EI mass spectra were obtained on a 4700 Proteome analyzer (MALDI-TOF-TOF) produced by ABI Company and on a HP 5989 mass spectra instrument, respectively. Hydrogen nuclear magnetic resonance spectra were determined on a GCT-TOF NMR spectrometer. Element analyses were performed on Perkin 2400 (II) autoanalyzer.

Linear absorption measurements of dilute solution (in THF, 1×10^{-6} mol dm^{-3}) have been measured with Hitachi U-3500 recording spectrophotometer from quartz cuvettes of 1 cm path.

* To whom correspondence should be addressed, wangxiaomei@mail.usts.edu.cn, xmduan@mail.ipc.ac.cn, and txt@sdu.edu.cn.
† Suzhou University of Science and Technology.
‡ Chinese Academy of Sciences.
§ Shandong University.

10.1021/jp1081005
Published on Web 12/29/2010

SCHEME 1: Synthetic Routes of the Branching Segments and Dendrimer Np-G1, Np-G2, and Np-G3[a]

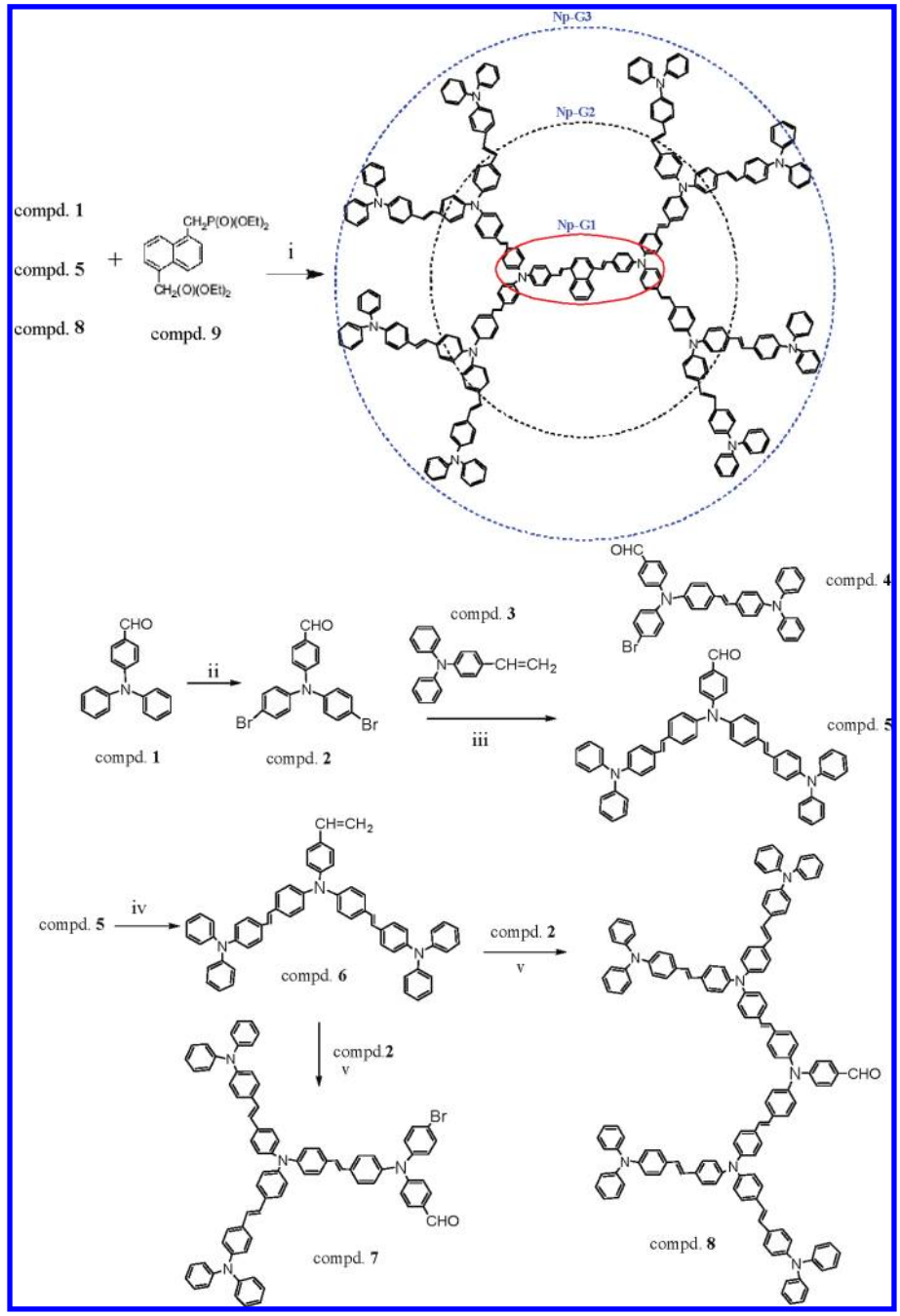

[a] (i) potassium *tert*-butoxide, dry THF, anhydrous and oxygen-free, reflux; (ii) Br_2, CH_2Cl_2, rt; (iii) $Pd(OAc)_2$, P(*o*-tolyl)$_3$, Et_3N/CH_3CN, 90 °C, 24 h; (iv) NaH, CH_3PPh_3I, THF, 60 °C; (v) $Pd(OAc)_2$, P(*o*-tolyl)$_3$, Et_3N/CH_3CN, 90 °C, 24 h.

Steady-state fluorescence and time-resolved decay curves were measured on an Edinburgh FLS 920 fluorophotometer equipped with time-correlated single-photon counting (TCSPC) card, while lifetime values were obtained by reconvolution fit analysis of the decay profiles with the aid of nF 900 software. In all fluorescence decay profiles, the monoexponential fit and dual-exponential fits give acceptable statistics parameters of $\chi^2 < 1.2$, where χ^2 is the "reduced chi-square" from the expression

$$\chi^2 = \sum_k W_k{}^2 \frac{[\chi_k - F_k]^2}{n}$$

One-photon fluorescence quantum yields (Φ_f) were measured using fluoresceine (in 0.1 mol dm^{-3} aqueous NaOH) as a standard. Fluorescence quantum yields (Φ_f) and lifetimes (τ_f) as well as the radiative ($k_f = \Phi_f/\tau_f$) and nonradiative ($k_{nr} = k_f(1 - \Phi_f)/\Phi_f$) decay constants are reported in Table 1.

Two-photon fluorescence (TPF) spectra are recorded by a fiber spectrometer (Ocean Optics USB2000 CCD), pumped by a Tsunami mode-locked Ti:sapphire system (700−880 nm, 80 MHz, <130 fs). A two-photon absorption (TPA) cross section (δ_{TPA}) was determined by two-photon fluorescence (TPF) method[35] based on eq 1

$$\delta_s = \delta_{ref} \frac{\Phi_{f(ref)}}{\Phi_{f(s)}} \frac{F_s}{F_{ref}} \frac{n_{ref}}{n_s} \frac{c_{ref}}{c_s} \quad (1)$$

TABLE 1: One-Photon Properties, Concluding Lifetime and Dynamics Constants, and Two-Photon Properties of Dendrimers[a]

				τ_f (ns)		k_f (10^8 s^{-1})		k_{nf} (10^8 s^{-1})			
dendrimer	λmax abs (nm)	λmax OPF (nm)	Φ_f	s-	l-	s-	l-	s-	l-	δ_{TPA}[b] (GM)	δ_{TPA}[c] (GM)
Np-G**1**	411	505	0.50	1.68		2.98		2.98		959	376
Np-G**1.5**	415	517	0.24	1.85	3.99	1.30	0.60	4.12	1.90	2802	565
Np-G**2**	412	526	0.31	1.79	2.91	1.73	1.07	3.85	2.38	5582	637
Np-G**2.5**	413	515	0.24	1.85	3.46	1.30	0.69	4.12	2.22	7846	889
Np-G**3**	415	503	0.22	1.69	3.15	1.30	0.70	4.61	2.48	9575	946

[a] Linear optical and two-photon measured concentrations in THF are at 1×10^{-6} and 1×10^{-4} M, respectively. [b] TPA cross sections at 700 nm (1 GM = 1×10^{-50} cm^4 s $photon^{-1}$). [c] TPA cross sections at 780 nm (1 GM = 1×10^{-50} cm^4 s $photon^{-1}$).

where the subscripts ref and s stand for reference (i.e, fluorescein) and samples, respectively. n, c, and F are the refractive index of solvent, solution concentration, and TPF integral, respectively. Φ_f represents the OPF quantum yield. The intensity of input pulses was confined within 0.5−2 GW/cm^2 in our experiment. The size of focusing spot (d) can be determined by the formula

$$d = \frac{4f\lambda M^2}{\pi D} \quad (2)$$

where f and λ are focus of the lens and wavelength of the laser beam, respectively, and M^2 and D are quality factor of the laser and the diameter of the laser beam before entering the lens, respectively. The experimental uncertainty amounts to 10%.

Cyclic voltammetry (CV) was employed to investigate the electrochemical behaviors of the emitting molecules. The CV curves in 0.10 M of tetrabutylammonium hexafluorophosphate (n-Bu_4NPF_6) and deoxygenated dichloromethane were obtained in a three-electrode cell, purged with N_2, with a platinum rod counter electrode, a glass carbon working electrode, and a Ag/AgCl (0.1 M) reference at a scan rate of 50 mV s^{-1}. HOMO (highest occupied molecular orbital) level relative to the vacuum level was calculated by using the oxidation potential (after being converted to the potential relative to the standard hydrogen electrode potential, NHE). The band gaps were obtained from the absorption spectra (absorption edge) of chromophores while the LUMO (lowest unoccupied molecular orbital) levels were calculated from the band gap and HOMO level.[36]

Two-Photon-Induced Polymerization. Photoresist resins, named R1, R1.5, R2, R2.5, and R3, respectively, are prepared by almost equal amounts of methyl methacrylate (MMA) and dipentaerythritol hexaacrylate (DEP-6A), wherein a small amount of initiator Np-G**1**, Np-G**1.5**, Np-G**2**, Np-G**2.5**, and Np-G**3**, respectively, was doped. As the control experiment, R_{benzil} was prepared by the similar description above instead of commercial benzil. Except for R2.5 and R3, all the photoresist resins are compatible, which can be polymerized successfully.

Two-photon polymerization (TPP) experiments were performed with the irradiation at 780 nm and 100 fs pulse from a mode-locked Ti−sapphire femtosecond laser (Tsunami, Spectra-Physics). The lasing source was tightly focused by a 100× oil immersion objective lens with a high numerical aperture (N.A. = 1.40, Olympus). The focal point was focused on the liquid photopolymerizable resin which was placed on a cover glass above the *xyz*-step motorized stage controlled by a computer. After laser fabrication, the unpolymerized resins were washed out with ethanol. The images of fabricated structures were observed using a field-emission scanning electron microscope (Hitachi, S-4300FEGd).

Results and Discussion

3.1. Synthesis. The synthetic routes of the branching segments and dendrimers (Np-G**1**, Np-G**2**, and Np-G**3**) are shown in Scheme 1. By the convergent approach, Np-G**1**, Np-G**2**, and Np-G**3** were obtained under the Wittig-type reaction of **9** and formyl compounds **1**, **5**, and **8**, respectively. Compounds[37] **4** and **5** were prepared in one pot by reaction of 4-(bis(4-bromophenyl)amino)benzaldehyde (**2**)[38] and *N*,*N*-diphenyl-4-vinylaniline (**3**)[38] under the Heck conditions. The aldehyde group in **5** was converted to vinylene group to obtain **6**[37] by the Wittig reaction with methyl phosphonium iodide in the presence of NaH as a base with 32% yield. **7** and **8** were obtained in one pot from **2** and **6** under palladium-catalyzed Heck conditions with 26% and 20% yields, respectively. As for half generation Np-G**1.5** and Np-G**2.5**, they were prepared by reaction of **9** with **4** and **7**, respectively.

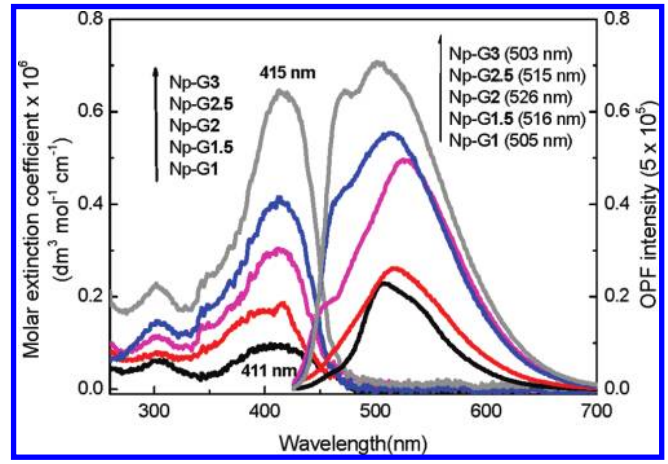

Figure 1. Linear absorption (left) and one-photon fluorescence (right) spectra of dendrimers in THF (1×10^{-6} mol·dm^{-3}).

All chromophores were purified by column chromatography and confirmed by ^1H NMR, mass spectra and elemental analysis. The pure initiators are soluble in common organic solvents such as chloroform and THF. Np-G**1**, Np-**1.5**, and Np-**G2** present very bright yellow color while Np-G**2.5** and Np-G**3** are yellow-green in powders.

3.2. One- and Two-Photon Properties. Linear absorption spectra of dendrimers are depicted in Figure 1 (left), wherein the strong absorption bands at ∼415 nm are attributed to intramolecular charge transfer (ICT) and bands at ∼300 nm are assigned to absorption of triphenylamine unit. The obvious enhancements in the molar absorbance for ICT bands from generation **1** to **3** suggest the increasing number of absorbing unit or strong intramolecular charge transfer (ICT) occurrence.

Under the excitation at ∼415 nm, strong one-photon fluorescence (OPF) was recorded in Figure 1 (right), wherein fluorescence intensity increases with generation number of the dendrimer, especially between Np-G**1.5** and Np-G**2**. Further increase is small. The red-shifted peaks from 505 nm (Np-G**1**) to 516 nm (Np-G**1.5**) to 526 nm (Np-G**2**) are observed; however, Np-G**2.5** (515 nm) and Np-G**3** (503 nm) are blue-shifted with

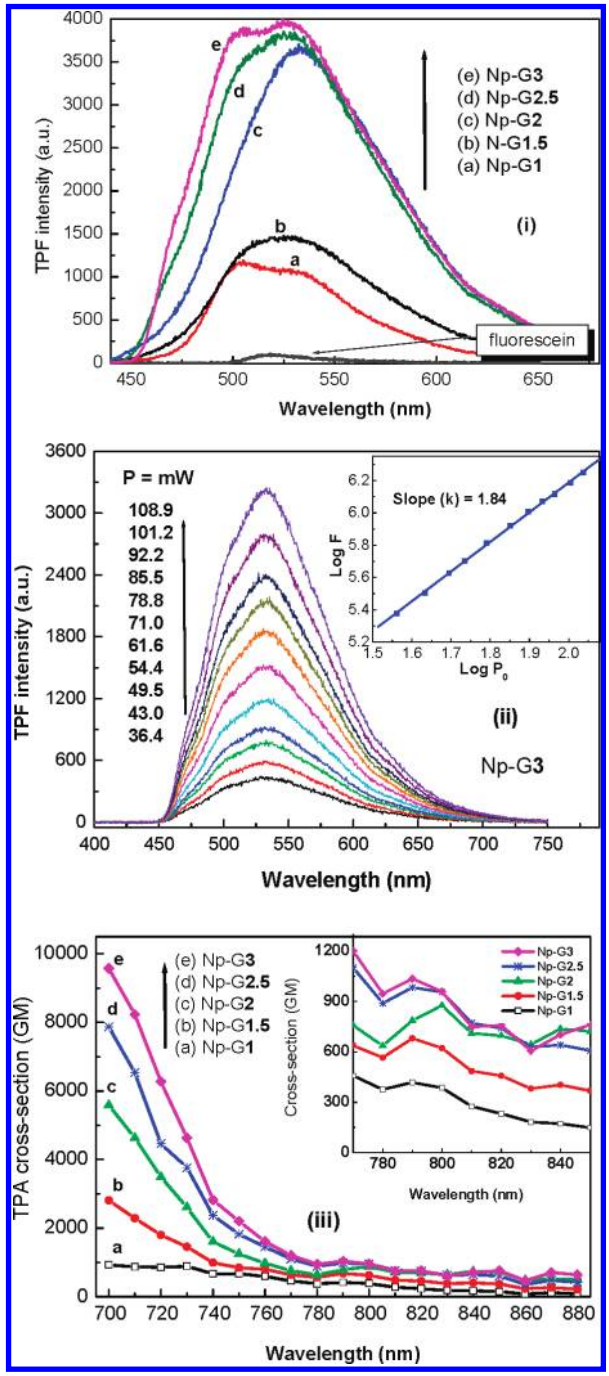

Figure 2. (i) Two-photon fluorescence (TPF) spectra under the same pumped powers at 700 nm. (ii) TPF spectra of Np-G**3** under different pumped powers at 800 nm, insert is the logarithmic plots of the fluorescence integral of chromophores versus different excitation intensities. (iii) Two-photon absorption cross sections of initiators in 700−880 nm regions.

the broadening and the shoulder (see Figure 1 right). Relative to the lower dendrimer, higher dendrimers (Np-G**2.5** and Np-G**3**) exhibit much different properties such as the compatibility with photoresist resins (mentioned above), the blue-shifted fluorescence (including OPF and TPF, see Figures 1 and 2i), and the negative dipole moment change, $\Delta\mu_{ge}$ (see Figure 3). These strongly suggest that the higher dendrimer possesses distinct structure in comparison with the small counterpart. One can speculate that higher dendrimers (Np-G**2.5** and Np-G**3**) might have a twisted configuration within the triphenylamine subunit,[39,40] with the result that the molecule has less complanation with limited π-electron delocalization. Thus, the fluo-

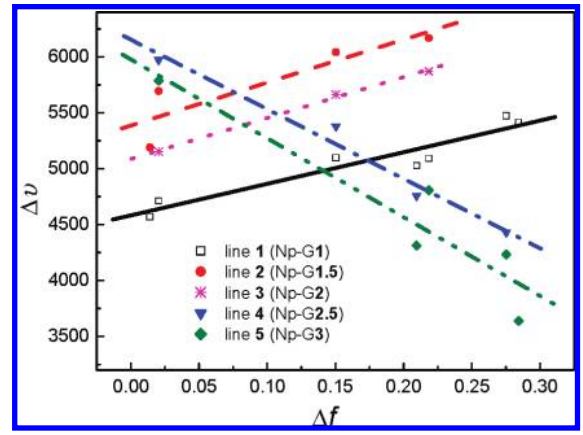

Figure 3. Lippert−Mataga relationship between the Stoke's shift $\Delta\nu$ ($\nu_{abs} - \nu_{em} = (\mu_e\Delta\mu_{ge}/\hbar c\alpha^3)\Delta f + C$) and orientation polarizability Δf ($(\varepsilon - 1)/(2\varepsilon + 1) - (n^2 - 1)/(2(2n^2 + 1))$) of solvents.

rescence peak was blue-shifted. With the generation number increasing, the total number of quantum levels should be increased. From this point of view, Figure 1 is understandable, in which the fluorescence band is broadened. Furthermore, the fluorescence shoulders of Np-G**2.5** and Np-G**3** attributed to triphenylamine segment[5] are also in agreement with the twisted configurations.

Two-photon fluorescence (TPF) spectra at the same pumped power under 700 nm excitation are presented in Figure 2 (i, wherein fluorescein reference is displayed for comparison). We presented TPF spectra at the wavelength of 700 nm because all molecular TPA cross sections show the highest in the range of 700−880 nm. (See Figure 3. Due to the limitation of our detecting equipment, we cannot observe the TPA peaks of initiators but expect that their strong TPA peaks may exist shorter than 700 nm.) Evidently, the TPF intensities are much higher than fluorescein and the TPF peaks are bathochromic shifted from Np-G**1** to Np-G**1.5** to Np-G**2**. For Np-G**2.5** and Np-G**3**, the blue-shifted TPF with shoulders suggests their twisted propeller-blade structures, which are in agreement with the corresponding OPF (see Figure 1). Two-photon fluorescence (TPF) spectra of Np-G**3** at different pumped powers under 800 nm excitation are presented in Figure 2(ii). The insert presents the logarithmic plot of the TPF integral versus the pumped power. The slope value obtained ($k = 1.84$), close to 2, indicates that two-photon absorption (TPA) is the main excitation mechanism in the femtosecond regime.[41] Here, we exhibited TPF spectra of Np-G**3** pumping with 800 nm for two reasons: (a) we would like to demonstrate that it was not single-photon-induced fluorescence but two-photon-induced fluorescence, which is proved by the insert of Figure 2(ii); (b) 800 nm is a commonly used wavelength in two-photon microfabrication.[17,19,42]

On the basis of the two-photon fluoescence (TPF) method,[35] TPA cross sections (δ_{TPA}) were calculated according to eq 1 and are displayed in Figure 2(iii). It can be seen that the TPA cross section (δmax TPA) at 700 nm shows significant enhancement from 959 GM (Np-G**1**) to 2802 GM (Np-G**1.5**) to 5582 GM (Np-G**2**) to 7846 GM (Np-G**2.5**) to 9575 GM (Np-G**3**). The δmax TPA values at 780 nm are also presented in the insert (Figure 2, iii) and Table 1. We reported that chromophores with enhancing TPA cross section were associated with larger dipole moment change ($\Delta\mu_{ge}$), originating from intramolecular charge transfer.[40] Herein, $\Delta\mu_{ge}$ values can be estimated according to the Lippert−Mataga relationship (see Figure 3), wherein the solid lines represent the fitting results of $\Delta\nu$ ($=\nu_{abs} - \nu_{em}$) and Δf (solvent polarizability). The slope (k) is proportional to the

TABLE 2: HOMO-LUMO and Energy Gap as Well as Two-Photon-Induced Polymerization Properties of Dendrimers

resins[a]			initiator						
name	solubility	initiator	HOMO/eV	LUMO/eV	ΔE/eV	wt %[b]	mmol %[c]	P_{th} /mW[d]	$R_p/\mu m^3\ s^{-1}$[e]
R1	soluble	Np-G**1**	−5.47	−2.90	2.57	0.20	0.30	2.3	0.45
R1.5	soluble	Np-G**1.5**	−5.46	−2.79	2.67	0.20	0.14	2.2	0.20
R2	soluble	Np-G**2**	−5.45	−2.77	2.68	0.20	0.11	1.1	1.33
R2.5	unsoluble	Np-G**2.5**	−5.45	−2.78	2.67				
R3	unsoluble	Np-G**3**	−5.45	−2.78	2.67				
R_{benzil}	soluble	benzil			4.1[f]	0.20	0.95	7.5	0.09

[a] The photoresist component is MMA/DEP-6A/initiator as 47.9/51.9/0.2 (wt %). [b] The weight (wt %) of initiators in the resins. [c] The millimolar (mmol %) concentration of initiators in the resins. [d] P_{th}, polymerization threshold. P_{th} value is defined as the average power before being induced into the objective lens, below which the polymer line cannot be fabricated using a linear scan speed of 10 μm s^{-1}. [e] R_p: polymerization rate at 2.4 mW laser power. [f] See ref 45.

value of $\mu_e\Delta\mu_{ge}/\alpha^3$. Since the molecular dimension (α) becomes larger with the generation number, the fact that slopes (k) are in the order of Np-G**2** > Np-G**1.5** > Np-G**1** implies the same sequence of dipole moment change ($\Delta\mu_{ge}$), that is, Np-G**2** > Np-G**1.5** > Np-G**1**. As for Np-G**2.5** and Np-G**3**, the negative slopes ($k < 0$) suggest that both dipole moments in the excited state (μ_e) are smaller than those in the ground state (μ_g). Because higher dendrimer with the twisted geometry (as discussed above) exhibits lower symmetry and poorer complanation, the polarity in the ground state (μ_g) is larger than that in the excited state (μ_e). Thus, the change in dipole moment between ground and excited state ($\Delta\mu_{ge} = \mu_e - \mu_g$) is negative. Nevertheless, the absolute values of dipole moment change ($|\Delta\mu_{ge}|$) are in the order of Np-G**3** > Np-G**2.5** > Np-G**2** > Np-G**1.5** > Np-G**1**. Clearly, the sequence of molecular dipole moment change ($\Delta\mu_{ge}$) accords with dendritic generation effect, which is shown to contribute to enhancement TPA cross section.

3.3. Two-Photon Polymerization (TPP) and Intermolecular Electron-Transfer between Initiator and Monomer. By the laser-scanning lithography (LSL) at 780 nm, photoresists R1, R1.5, and R2 (see Table 2) can be effectively two-photon-polymerized only occurrence near the vicinity of a focal point of a laser beam. In the part out of the laser focus, the polymerization reaction did not take place and the photoresists are easily washed out by ethanol. Thus, a variety of micro-objects including micro-ox (15 μm × 10 μm bulk size) and 3D photonic crystal (20 μm × 20 μm bulk size) can be successfully fabricated with a spatial resolution of scale to approximately 500 nm. As shown in Figure 4, the diamond structures are very regular, indicating these dendritic initiators exhibit potential application in TPP 3D microfabrication.

We investigated the two-photon polymerization (TPP) rate (R_p) and threshold powers (P_{th}), which are correlated with the efficiency and sensitivity, respectively, of the photoresist resins containing different initiators. Using the equation $R_p = \pi (d/2)^2 \nu_s$ (where π is the width of the line fabricated and ν_s is the linear scan speed[42−44]), the plots of TPP rate vs laser power are presented in Figure 5. As outlined in Table 2, the R_p values of R1, R1.5, and R2 were found to be 0.45, 0.20, and 1.33 $\mu m^3\ s^{-1}$ in the case of the laser power 2.4 mW, respectively. Among them, resin R2 contained Np-G**2** as initiator was the most efficient. However, when laser power is at 2.4 mW, R_{benzil} cannot be polymerized. On the other hand, the P_{th} values of R1−R2 are measured to be are 2.3, 2.2, and 1.2 mW, respectively, which are much lower than that of R_{benzil} (P_{th}=7.5 mW). These strongly suggest that the dendritic initiator presents a higher sensitivity than the conventional initiator, benzil, and also display the enhancement in sensitivity with the generation number.

It was stressed that TPP rates (R_p) and threshold (P_{th}) are compared when the initiator was doped at the weight concentration of 0.2%. If the doped amounts are converted to molar concentrations (mmol %), the polymerization sensivity and efficiency would be enhanced with the generation number. For example, at the almost samne threshold powers (P_{th} = ∼2.3 mW), the resins R1 and R1.5, containing 0.30% (mmol %) of Np-G**1** and 0.14% (mmol %) of Np-G**1.5**, respectively, present polymerization rates of 0.45 and 0.20 $\mu m^3 s^{-1}$, respectively (see

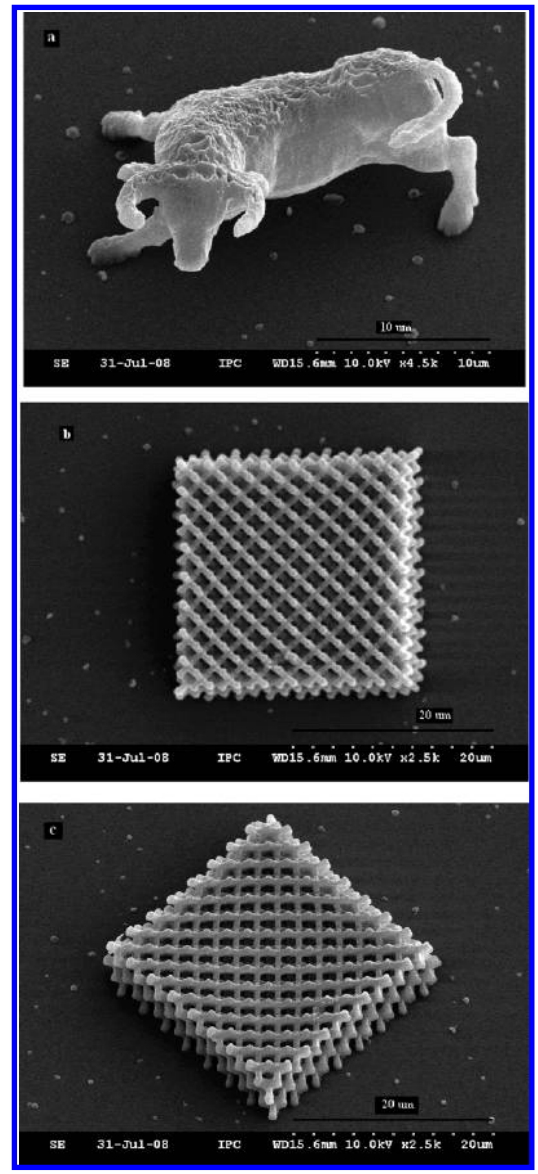

Figure 4. SEM images of microstructures fabricated by TPP using Np-G**2** as initiator at the scan speed is 10 $\mu m\ s^{-1}$: (a) micro-ox ox; (b and c) 3D diamond photonic crystal.

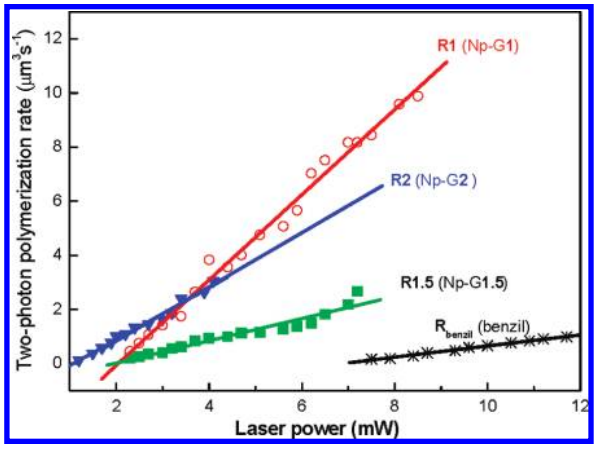

Figure 5. The dependence of polymerization rates upon laser power for photoresists containing the same weight doped concentration (wt % = 0.2%) of initiators.

Table 2). One can deduce that under these conditions if Np-G**1** and Np-G**1.5** were doped at the same molar concentrations, samller P_{th} and larger R_p values for resin R1.5 would be obtained, relative to R1. By the extrapolation, the TPP efficiency is increased with the initiator' generation number.

The overall TPP approach involved in two-photon excitation, intramolecular charge transfer, and intramolecular energy transfer as well as intermolecular electron transer are described in Figure 6. The possible intramolecular light energy-transfer processes within dendrimer topology was from the periphery unit to the center. As presented in Table 2 and Table 3, generation **1** (Np-G**1**) possesses the smallest energy level difference (ΔE = 2.57 eV) among all the dendrimers (ΔE = ~2.67 eV), and the triphenylamine-branching segments show the largest HOMO−LUMO differences (ΔE = 2.76−2.86 eV). Thus, the light energy can be absorbed by the peripheral triphenylamine unit and then smoothly transferred toward the trap center (i.e., generation **1**) that acts as the energy funnel. This can be confirmed by the fact that all the dendrimenrs present the fluorescence peaks at 503−526 nm, similar to generation **1** (505 nm), which show much lower than the branching segments (453−462 nm). Also, an obvious fluorescence enhancement of Np-G**3** was recorded on the excitation of **8**, compared to direct excitation of Np-G**3** or Np-G**1,** revealing that the emission of dendrimer is not from their branching segments but mainly from generation **1**. Fluorescence decay dynamics have demonstrated (see Table 1) that the generation **1** gives the monolifetime (1.68 ns) while the higher dendrimers possess the dual lifetimes (~1.68 ns, 3−4 ns). The short lifetimes (~1.68 ns) are attributed to the decay of generation **1** (the trap center of the energy funnel) and the long lifetimes (3−4 ns) correspond to the decay of intramolecular charge-tranfer (ICT) or enegry-transfer (IET), which prolongate the nonradiative approach (k_{nf} = (3.85−4.61) × 10^8 s^{-1}), relative to generation **1** (k_{nf} = 2.98 × 10^8 s^{-1}). These would have contribution to the photochemistry process and lead to high TPP sensitivity and efficiency.

TABLE 3: Linear Optical Properties and Energy Level of Triphenylamine-Branching Segments

compd	λ_{max}^{abs},nm	λ_{max}^{abs},nm	Φ_f	E_{HOMO}, eV	E_{LUMO}, eV	ΔE, eV
4	386	453	0.67	−5.75	−2.89	2.86
6	392	454	0.45	−5.55	−2.76	2.79
7	403	456		−5.64	−2.88	2.76
8	397	462	0.35	−5.67	−2.91	2.76

With an acrylate matrix that contained the dendritic initiator, the interaction between them can be observed in Figure 7, wherein the fluorescence excitation and emission spectra of initiators in the presence of acrylate (MMA:DEP-6*A* = 1:1, v/v) were presented. At first, the fluorescence excitation spectra of initiators display dual-fluorescence shapes (see Figure 7A,C,E,G) that correspond to their respective absorption spectra (see Figure 1, left). When the concentration of acrylate was increased to ~80%, the dual-fluorescence excitation spectra were deformed to single fluorescence spectra. On the other hand, the fluorescence emissions are enhanced when a small amount of acrylate was added (see Figure 7B,D,F,H), which is interpreted as the molecular rotation suppressing and the complanation resulting from the solvent viscosity. However, when acrylate concentration was increased to ~80%, the fluorescence emission is sharply decreased accompanying a blue-shifted peak and deformed shape. The partial fluorescence quenching would be

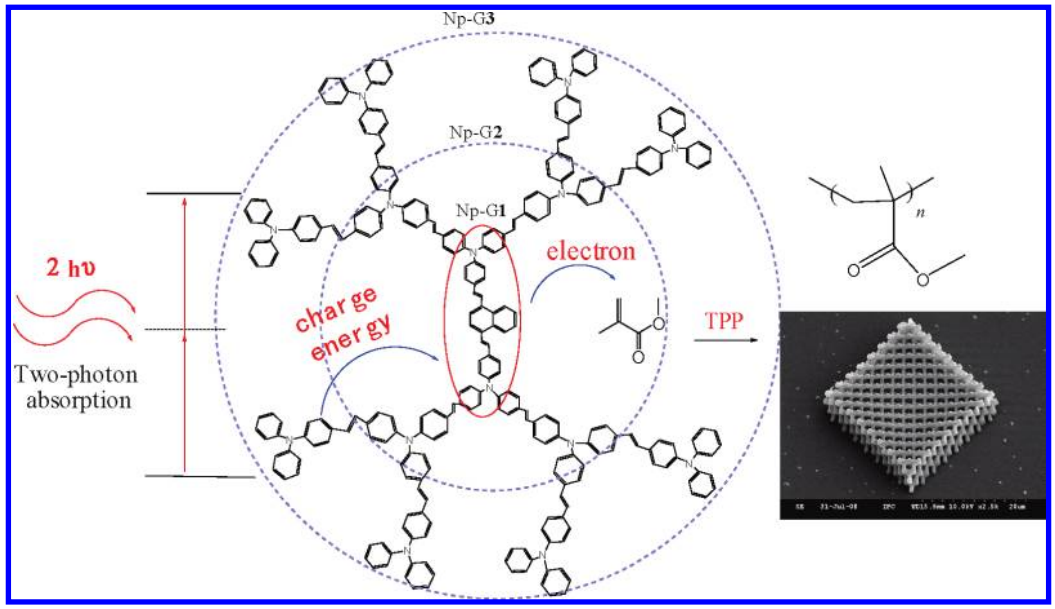

Figure 6. The overall TPP approach involved in TPA, intramolecular charge transfer, and intramolecular energy transfer as well as intermolecular electron transfer.

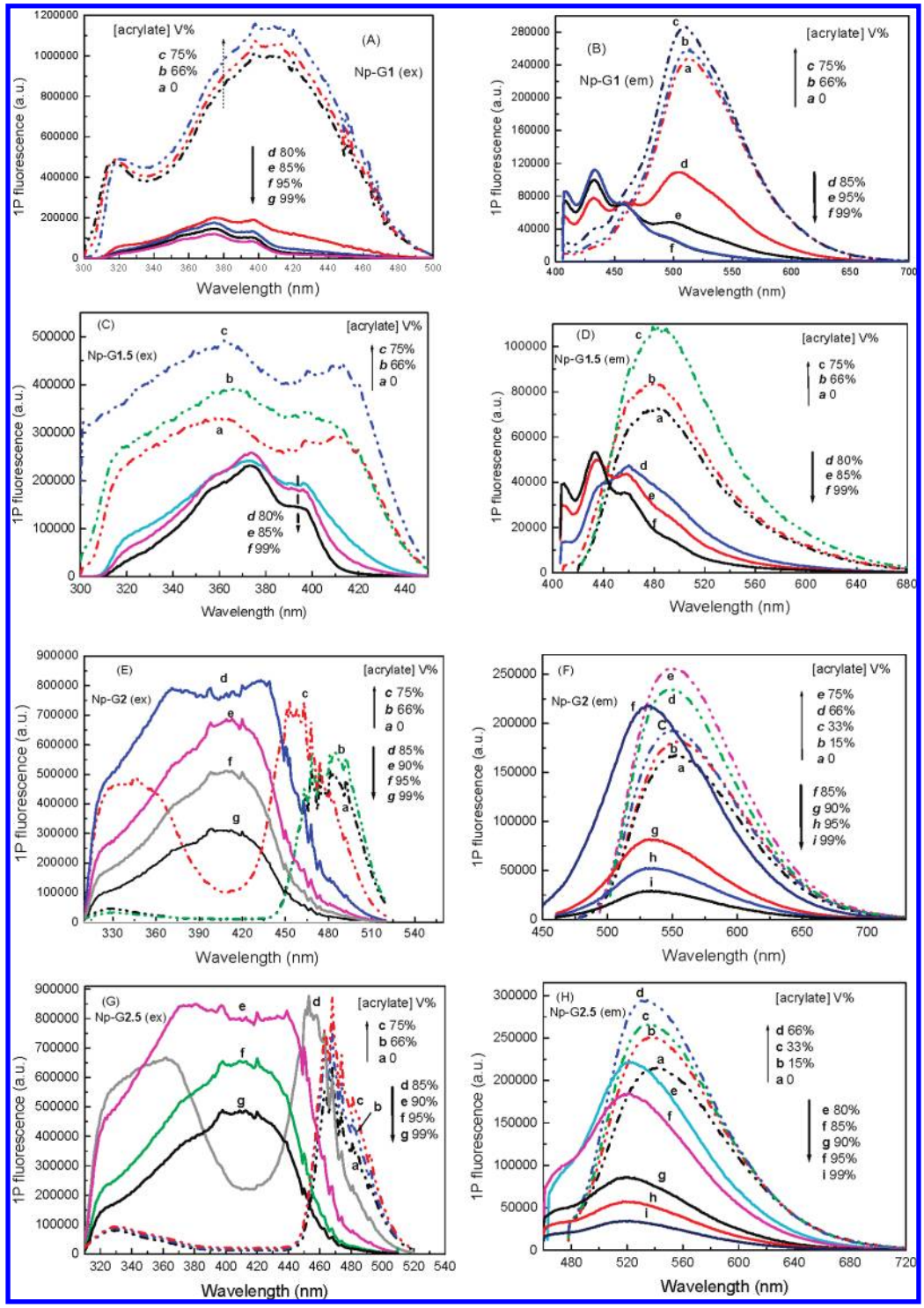

Figure 7. Fluorescence excitation (A, C, E, G) and emission (B, D, F, H) spectra of dendrimers in the presence of acrylate monomer with different concentrations.

expected to be the consequence of strong interaction between monomer and initiator.[45,46]

It was reported that the two-photon-induced polymerization of acrylate monomer proceeds to the mechanism via either energy transfer or electron transfer[31] or charge transfer[20] between initiator and monomer. The energy transfer from the our initiator to methacrylate based monomer is forbidden because the LUMO−HOMO difference (ΔE) of dendritic initiators (~2.60 eV) is less than that of monomer MMA (4.1 eV)[45] (see Table 2). Cyclic voltammetry (CV) curves of dendrimers exhibit different separate waves during an anodic scan (see Figure 8), corresponding to the oxidation of the neutral species (wave 1) and the oxidation of the resulting radical cations (wave 2 and wave 3), respectively. More importantly, both oxidation and reduction waves occur at the positive potential regions, revealing that these dendrimers easily lose the electron and the corresponding cations are excited to obtain a diradical conformation in their excited states. Furthermore, one can see that the first oxidation potentials of dendrimers are decreased with the generation number, that is, in the order of Np-G**1** (732 mV)

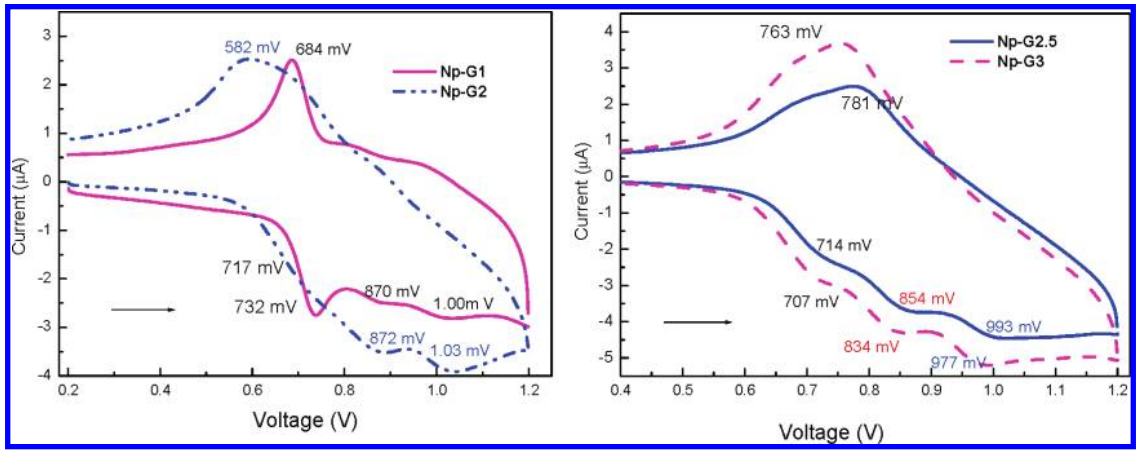

Figure 8. Cyclic voltammogram of dendrimers in deoxygenated CH_2Cl_2, purged with nitrogen, containing 0.1 M of tetrabutylammonium hexafluorophosphate (n-Bu_4NPF_6), scan rate of 50 mV s^{-1}.

> Np-G**2** (717 mV) > Np-G**2.5** (714 mV) > Np-G**3** (707 mV). The reduced oxidation potentials imply that higher dendrimers are prone to lose electrons and the observed decrease of the oxidation potentials is also in agreement with the enhancement in TPP efficiency and sensitivity, which support the mechanism of electron transfer from initiator to monomer on the basis of the Marcus theory.[47−49] Thus, on the assumption that the dendritic initiator first produces the excited state via two-photon absorption, following transport of the energy from the triphenylamine-branching to the generation **1** (energy funnel), and then transfers an electron toward the acrylate monomer, and finally induces the later to polymerize, as described in Figure 6.

Conclusions

We have synthesized a new family of conjugated dendritic donors feeding into a central naphthalene unit, which exhibit increasing two-photon absorption cross section (δ_{TPA}) from 959 to 9575 GM with the generation number from **1** to **3**. These dendrimers showed the strong relevancy between intramolecular charge transfers and TPA cross section (δ_{TPA}) and have successfully initiated the acrylate resin to two-photon-polymerized.

The photochemical processes within the dendritic topology that the light energy was absorbed by the peripheral triphenylamine unit and then transferred to the trap center (generation **1**) were described. Fluorescence decay dynamics have demonstrated that generation **1** gives the monolifetime (1.68 ns) while the higher dendrimers possess the dual lifetimes (∼1.68 and 3−4 ns). The short lifetime was attibuted to the decay of generation **1** (the trap center of energy funnel), and the long lifetimes correspond to the decay of intramolecular charge tranfer (ICT) or enegry transfer (IET), which prolongate the nonradiative approach ($k_{nf} = (3.85-4.61) \times 10^8$ s^{-1}), relative to generation **1** ($k_{nf} = 2.98 \times 10^8$ s^{-1}). Although the strong interaction between dentritic initiator and monomer has been observed by fluorescecne quenching measurements, no intermolecular energy transfer is observed but intermolecualr electron transfer is confirmed. With the generation number, electron-rich dendrimer possesses easily electron-transfer character with the oxidation potentials decreasing in the oeder of Np-G**1** (732 mV) > Np-G**2** (717 mV) > Np-G**2.5** (714 mV) > Np-G**3** (707 mV), which are in agreement with the enhancement in TPP efficiency and sensitivity. Thus, on the assumption that dendritic initiator first produces the excited state via two-photon absorption, the energy moves from the triphenylamine branching to generation **1** (energy funnel) and then transfers the electron toward the acrylate monomer, and finally induces the later to polymerize.

Acknowledgment. The authors are grateful to the National Natural Science Foundation of China (Grant Nos. 50673070, 50973077, 21071107, and 50773091), Key Project of Chinese Ministry of Education (No. 204053), The National Basic Research Program of China (2010CB934103), and Science and Technology Development Project of Suzhou (SYJG0931) for financial support.

Supporting Information Available: Details of compound synthesis. This information is available free of charge via the Internet at http://pubs.acs.org.

References and Notes

(1) He, G. S.; Tan, L. S.; Zheng, Q. D.; et al. *Chem. Rev.* **2008**, *108*, 1245.
(2) He, G. S.; Kim, K. S.; Chung, S. J.; et al. *Chem. Mater.* **2000**, *12*, 2838.
(3) Chung, S. J.; Kim, K. S.; Lin, T. C.; He, G. S.; et al. *J. Phys. Chem. B* **1999**, *103*, 10741.
(4) Chung, S. J.; Lin, T. C.; Kim, K. S.; He, G. S.; et al. *Chem. Mater.* **2001**, *13*, 4071.
(5) Wang, X. M.; Yang, P.; Li, B.; et al. *Chem. Phys. Lett.* **2006**, *424*, 333.
(6) Lee, H. J.; Sohn, J.; Hwang, J.; et al. *Chem. Mater.* **2004**, *16*, 456.
(7) Katan, C.; Terenziani, F.; Mongin, O.; et al. *J. Phys. Chem. A* **2005**, *109*, 3024.
(8) Wang, Z. M.; Wang, X. M.; Zhao, J. F.; et al. *Dyes Pigm.* **2009**, *79*, 145.
(9) He, G. S.; Przemyslaw, P. M.; Prasad, P. N.; et al. *Nature* **2002**, *415*, 767.
(10) Bhawalkar, J. D.; He, G. S.; Prasad, P. N. *Rep. Prog. Phys.* **1996**, *59*, 1041.
(11) Lee, K. S.; Yang, D. Y.; Park, S. H.; et al. *Polym. Adv. Technol.* **2006**, *17*, 71.
(12) Lee, K. S.; Kim, R. H.; Cho, N. *SPIE Newsroom* **2008**, *20*, doi: 10.1117/2.1200801.0962.
(13) Tanaka, T.; Ishikawa, A.; Kawata, S. *Appl. Phys. Lett.* **2006**, *88*, 081107-3, doi:10.1063/1.2177636.
(14) Kosei, U.; Saulius, J.; Toshiyuki, S.; et al. *J. Am. Chem. Soc.* **2008**, *130*, 6928.
(15) Stephanie, A.; Paul, V. B. *Adv. Funct. Mater.* **2005**, *15*, 1995.
(16) Erik, C. N.; Florencio, G. S.; Paul, V. B. *Adv. Funct. Mater.* **2008**, *18*, 1983.
(17) Gu, J.; Wang, Y. L.; Chen, W. Q.; et al. *New J. Chem.* **2007**, *31*, 63.
(18) Lee, K. S.; Yang, D. Y.; Park, S. H.; et al. *Polym. Adv. Technol.* **2006**, *17*, 72.
(19) Xing, J. F.; Chen, W. Q.; Gu, J.; et al. *J. Mater. Chem.* **2007**, *17*, 1433.

(20) Wang, X. M.; Jin, F.; Zhang, W. Z.; et al. *Dye Pigments* **2011**, *88*, 57.
(21) Laurent, P.; Olivier, M.; Claudine, K.; et al. *Org. Lett.* **2004**, *6*, 47.
(22) Wang, X. M.; Yang, P.; Xu, G. B.; et al. *Synth. Met.* **2005**, *155*, 464.
(23) Wang, Z. M.; Wang, X. M.; Zhao, J. F.; et al. *Dyes Pigm.* **2008**, *79*, 145.
(24) Wang, D. Q.; Wang, X. M.; He, Q. G.; et al. *Tetrahedron Lett.* **2008**, *49*, 5871.
(25) Cho, B. R.; Son, K. H.; Lee, S. H.; et al. *J. Am. Chem. Soc.* **2001**, *123*, 10039.
(26) Belfield, K. D.; Katherine, J. S.; liu, Y.; et al. *J. Phys. Org. Chem.* **2000**, *13*, 837.
(27) Bratton, D.; Yang, D.; Dai, J. Y.; et al. *Polym. Adv. Technol.* **2006**, *17*, 94.
(28) Lee, K. S.; Yang, D. Y.; Park, S. H.; et al. *Polym. Adv. Technol.* **2006**, *17*, 72.
(29) Watanabe, T.; Akiyama, M.; Totani, K.; et al. *Adv. Funct. Mater* **2002**, *12*, 611.
(30) Dong, Y.; Yu, X. Q.; Sun, Y. M.; et al. *Polym. Adv. Technol.* **2007**, *18*, 519.
(31) Cumpston, B. H.; Ananthavel, S. P.; Barlow, S.; et al. *Nature* **1999**, *398*, 51.
(32) Drobizhev, M.; Rebane, A.; Sigel, C.; et al. *Chem. Phys. Lett.* **2000**, *325*, 375.
(33) Stewart, G. M.; Fox, M. A. *J. Am. Chem. Soc.* **1996**, *118*, 4354.
(34) Kopelman, R.; Shortreed, M.; Shi, Z. Y.; et al. *Phys. Rev. Lett.* **1997**, *78*, 1239.
(35) Albota, M. A.; Xu, C.; Webb, W. W. *Appl. Opt.* **1998**, *37*, 7352.
(36) Xia, C. Y.; Wang, X. M.; Lin, J.; et al. *Synth. Met.* **2009**, *159*, 194.
(37) Huang, Z. Z.; Wang, X. M.; Li, B.; et al. *Opt. Mater.* **2007**, *29*, 1084.
(38) Chung, S. J.; Lin, T. C.; Kim, K. S.; He, G. S.; et al. *Chem. Mater.* **2001**, *13*, 4071.
(39) Drobizhev, M.; Karotki, A.; Dzenis, Y.; et al. *J. Phys. Chem. B* **2003**, *107*, 7540.
(40) Wang, X. M.; Wang, D.; Zhou, G. Y.; et al. *J. Mater. Chem.* **2001**, *11*, 1600.
(41) Zhao, Y.; Li, X.; Wu, F.; et al. *J. Photochem. Photobiol., A* **2006**, *177*, 12.
(42) Duan, X.-M.; Wada, T.; Okada, S.; et al. *MRS Symp. Proc.* **2000**, *581*, 31.
(43) Lu, Y. M.; Hasegawa, F.; Ohkuma, S.; et al. *J. Mater. Chem.* **2004**, *14*, 1391.
(44) Lu, Y. M.; Hasegawa, F.; Ohkuma, S.; et al. *J. Mater. Chem.* **2004**, *14*, 75.
(45) Nicholas, C. S.; Anzar, K.; Shannon, W. B.; et al. *J. Am. Chem. Soc.* **2008**, *130*, 8280.
(46) Nguyen, L. H.; Straub, M.; Gu, M. *Adv.Funct. Mater.* **2005**, *15*, 209.
(47) Kavarnos, G. J.; Turro, N. J. *Chem. Rev.* **1986**, *86*, 401.
(48) Marcus, R. A.; Sutin, N. *Biochim. Biophys. Acta* **1985**, *811*, 265.
(49) Bi, Y. B.; Neckers, D. C. *Macromolecules* **1994**, *27*, 3683.
(50) Li, W. L.; Wang, X. M.; Jiang, W. L.; et al. *Dyes Pigm.* **2008**, *76*, 485.
(51) Wang, X. M.; Zhou, Y. F.; Yu, W. T.; et al. *J. Mater. Chem.* **2000**, *10*, 2698.

JP1081005